Differentiation of Complex Lipid Isomers by Radical-Directed Dissociation Mass Spectrometry

Huong T. Pham,[†,§,¶] Tony Ly,[†,¶] Adam J. Trevitt,[†] Todd W. Mitchell,[‡] and Stephen J. Blanksby*[,†]

[†]ARC Centre of Excellence for Free Radical Chemistry and Biotechnology, School of Chemistry, University of Wollongong, Wollongong, NSW 2522, Australia

[‡]School of Health Sciences, University of Wollongong, Wollongong, NSW 2522, Australia

Ⓢ *Supporting Information*

ABSTRACT: Contemporary lipidomics protocols are dependent on conventional tandem mass spectrometry for lipid identification. This approach is extremely powerful for determining lipid class and identifying the number of carbons and the degree of unsaturation of any acyl-chain substituents. Such analyses are however, blind to isomeric variants arising from different carbon–carbon bonding motifs within these chains including double bond position, chain branching, and cyclic structures. This limitation arises from the fact that conventional, low energy collision-induced dissociation of even-electron lipid ions does not give rise to product ions from intrachain fragmentation of the fatty acyl moieties. To overcome this limitation, we have applied radical-directed dissociation (RDD) to the study of lipids for the first time. In this approach, bifunctional molecules that contain a photocaged radical initiator and a lipid-adducting group, such as 4-iodoaniline and 4-iodobenzoic acid, are used to form noncovalent complexes (i.e., adduct ions) with a lipid during electrospray ionization. Laser irradiation of these complexes at UV wavelengths (266 nm) cleaves the carbon–iodine bond to liberate a highly reactive phenyl radical. Subsequent activation of the nascent radical ions results in RDD with significant intrachain fragmentation of acyl moieties. This approach provides diagnostic fragments that are associated with the double bond position and the positions of chain-branching in glycerophospholipids, sphingomyelins and triacylglycerols and thus can be used to differentiate isomeric lipids differing only in such motifs. RDD is demonstrated for well-defined lipid standards and also reveals lipid structural diversity in olive oil and human very-low density lipoprotein.
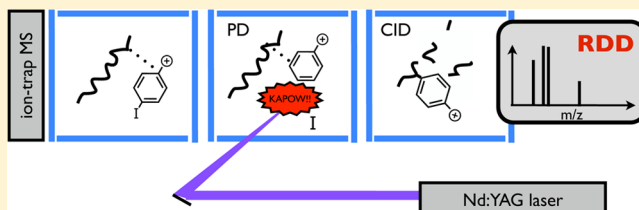
In biology, complex lipids serve numerous important functions that can be broadly categorized as energy storage (e.g., triacylglycerols in adipose tissues),[1] structural building blocks (e.g., glycerophospholipids in membrane bilayers),[2,3] and signaling molecules (e.g., diacylglycerols and ceramides).[4,5] In all cases, the ability of an individual lipid (or class of lipids) to perform its biochemical role is dependent on its molecular structure. For example, phospholipids with different headgroups distribute specifically within the cell and play an important role in lipid–sterol interactions that affect the structure of membrane bilayers.[6] Similarly, the impacts of the degree of unsaturation and the presence of chain branching in lipid acyl chains on membrane fluidity are well-known.[7−9] Recent studies highlight the significance of double bond position in dictating interactions between phospholipids and cholesterol, demonstrating that this subtle structural feature can affect membrane order.[7,10] The extensive decoration of phospholipid headgroups are often reported as the key molecular recognition features, such as the polysaccharide moieties present in glycophosphatidylinositols, glycoceramides, and their derivatives.[3] Increasingly however, the specific role of the hydrophobic lipid tail is being recognized as critical to lipid–protein binding and, in some instances, establishing the correct presentation of the headgroup for subsequent molecular-recognition events. In numerous crystal structures of the protein receptor SF-1 for example, the acyl chain positions, chain length and even double bond position appear to be much more significant to phospholipid–protein binding than the polar lipid headgroup.[11−13] Similarly, extensive work on the structure−activity relationships between lipid antigens and the CD1 family of glycoproteins points to the importance of acyl chain length, relative acyl chain position, chain branching,[14] and even stereochemistry (i.e., cis versus trans)[15] in both binding and bioactivity.[16] The importance of elucidating acyl chain structure in complex lipids to inform our understanding both their structural and signaling functions is thus becoming increasingly apparent.

Electrospray ionization tandem mass spectrometry has a preeminent place as a fast and sensitive method for analysis of individual lipids within biological lipid extracts.[17] In this approach, even-electron lipid ions are generated by electrospray ionization (ESI) of a crude lipid extract or chromatographic effluent. Pseudomolecular ions are then mass-selected and subjected to collision-induced dissociation (CID) to provide structural information. For most complex lipids, the combination

of intact mass and CID product ions can be used to derive lipid class along with the number of carbons and the degree of unsaturation in each of the acyl chains. As such, this approach is widely and effectively deployed in protocols for the identification of various classes of complex lipids including glycerophospholipids (GPs), sphingomyelins (SMs), and triacylglycerols (TGs). The low energy (<100 eV) CID spectra of complex lipids are relatively simple with most of the ion signal concentrated in a few abundant product ions commonly arising from heterolytic dissociation adjacent to the headgroup or at the ester/amide linkages.[18] While this relative simplicity aids in the assignment of the gross structural features of the lipid, little structural insight is gained into the C−C bonding motifs within the acyl chains themselves. As a result, the low energy CID spectra of isomeric lipids that differ only in double bond position or stereochemistry, chain branching, or cyclic structures are identical (for examples see refs 19 and 20).

Intrachain fragmentation in ionized complex lipids can be induced by employing either (i) higher collision energies (>keV) on sector type[21] (and more recently tandem time-of-flight[22]) mass spectrometers or (ii) multistage CID (MS[n]) on ion-trap platforms.[23,24] The broader application of these approaches appears to have been limited by the incompatibility of the high energy platforms with ESI and the low sensitivity of the multistage approach. It is noted however, that the latter has been recently improved through the use of time-aligned-CID spectra on an ion-mobility capable quadrupole time-of-flight mass spectrometer.[25] Alternative approaches to the elucidation of double bond position in complex lipids have evolved that exploit selective ion−molecule chemistry (e.g., covalent adduct chemical ionization and ozone induced dissociation[26,27]) but these cannot be generalized to other motifs such as chain branching points. In contrast to the CID behaviors of even-electron ions, radical ions produced by traditional electron ionization (EI) of lipids give rise to extensive intrachain fragmentation albeit on simple lipids, such as fatty acids and their derivatives.[28] With appropriate control of internal energy either by derivatization;[29,30] low electron energy (30 eV);[31] or employing CID on molecular ions formed under EI (so-called EI-CID)[32,33] detailed structure elucidation of lipids including position(s) of double bonds and chain branching has been undertaken. While powerful, these EI protocols cannot be extrapolated to complex lipids that have both limited vapor pressure and thermal stability.

Contemporary mass spectrometric methods from the proteomics community generate radical ions from their even-electron counterparts by electron transfer to multiply charged ions. Such approaches have also been applied to lipids[34,35] but have not been extensively deployed because lipidomic analyses are mostly concerned with singly charged ions. An alternative approach to the generation of radical ions from even electron peptides and proteins is known as radical-directed dissociation (RDD).[36] In this method, a photocaged radical precursor is attached to the analytical target and irradiation of the precursor in the mass spectrometer "uncages" the radical with subsequent CID of the nascent radical ion yielding radical driven fragmentation of the precursor. Herein, two photocaged radical precursors, 4-iodobenzoate (IB), and 4-iodoaniline (IA), are described that include a UV-labile carbon−iodine bond and a para-substituted functional group that has been selected to bind noncovalently to complex lipids. RDD of these noncovalent complexes are shown to yield fragmentation diagnostic of lipid structure.
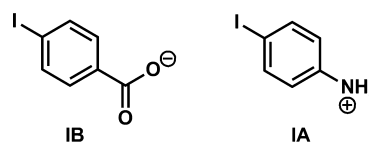
MATERIALS AND METHODS

All reagents and synthetic lipid standards were commercially available and were used without further purification. Full details are provided as Supporting Information. Spanish olive oil (Always Fresh, Riviana Foods Pty Ltd., Australia) was purchased from a local food store. Total triacylglycerol (TG) extracts from very-low density lipoprotein (VLDL) had previously been prepared.[37,38] Sample preparation is facile, generally requiring only mixing of the lipid and the adducting reagent in methanol in concentrations of ~10−15 μM lipid and ~20−30 μM adducting reagent. For phosphatidylcholine (PC) and sphingomyelin (SM) experiments, concentrations of 15 μM lipid and 30 μM 4-iodobenzoic acid (IB) were used. TG samples (i.e., TG standards, olive oil and VLDL samples) contained final concentration of ~10 μM TGs and 20 μM 4-iodoaniline (IA) in presence of 0.5% formic acid to aid the formation of protonated iodoaniline for charge adducting. The sample solutions were introduced into an electrospray ionization mass spectrometer by direct infusion to generate the gaseous noncovalent complexes $[PC + IB]^-$, $[SM + IB]^-$, or $[TG + IA]^+$. Experiments were performed using an electrospray ionization linear ion-trap mass spectrometer (Thermo Fisher Scientific LTQ, San Jose, California). The linear ion trap has been modified as previously described to enable photodissociation experiments.[39] A summary of these modifications and instrument operating conditions are provided as Supporting Information.

RESULTS AND DISCUSSION

ESI of methanolic solutions containing PC(9Z-18:1/9Z-18:1) and 4-iodobenzoic acid yield two major peaks in the mass spectrum corresponding to 4-iodobenzoate $[IB^-]$ and the noncovalent complex $[PC + IB]^-$. Such adduct ions are analogous to the formate and acetate complexes widely used in PC analysis,[40,41] and the CID spectrum of $[PC + IB]^-$ ions are also consistent with prior reports of carboxylate adducts showing predominantly demethylated phosphatidylcholine $[PC − CH_3]^-$ via loss of methyl iodobenzoate (see Supporting Information, Figure S1a,b).[42] In contrast, photodissociation of the $[PC + IB]^-$ (m/z 1032) at 266 nm yields a major product ion at m/z 905 arising from the loss of atomic iodine (Figure 1a). Cleavage of the carbon−iodine bond in this process initially generates a reactive phenyl radical within the complex (Scheme 1). Given the reactivity of the nascent phenyl radical, abstraction of a hydrogen atom from the PC is exothermic and thus likely to be facile (i.e., the C−H bond dissociation energy in benzene is 112.9 kcal mol^{−1} while aliphatic C−H bonds are <98.4 kcal mol^{−1}).[43] Evidence for H-abstraction is provided by the CID spectrum of m/z 905 (Figure 1b) that is dominated by neutral loss of methyl benzoate resulting in a $[PC − CH_3 − H]^{\bullet -}$ radical anion at m/z 769. Subsequent CID of the m/z 769 (Figure 1c) yields both even-electron product ions, analogous to those derived from CID of the even-electron $[PC - CH_3]^-$ precursor ion at m/z 770 (Figure 1d), but also a richer fragmentation that includes carbon−carbon bond dissociation along the alkenyl chain. The presence of well-recognized product ions in Figure 1(c), such as those derived from neutral losses of the 18:1 fatty acyl chains
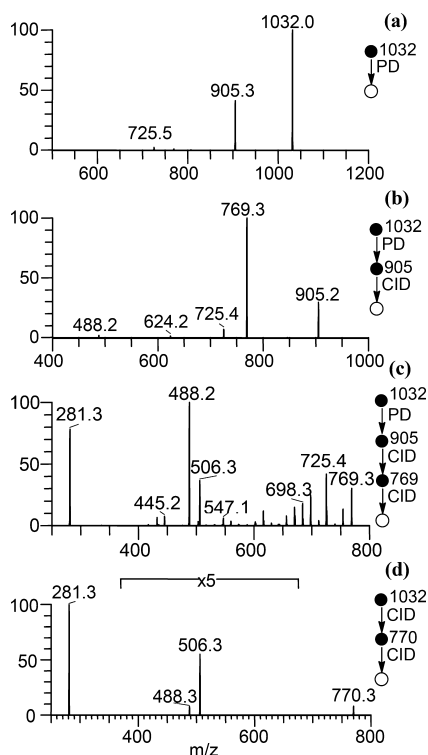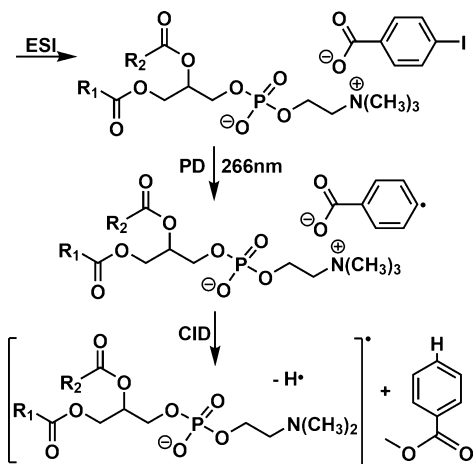
Figure 1. (a) PD (266 nm) of the [PC(9Z-18:1/9Z-18:1) + IB]⁻ complex at m/z 1032. (b) CID of the resulting [PC(9Z-18:1/9Z-18:1) + IB − I]•⁻ at m/z 905. (c) Subsequent CID of [PC − CH₃ − H]•⁻ at m/z 769 results in the RDD spectrum. (d) CID of the even-electron [PC − CH₃]⁻ ion at m/z 770.

Scheme 1. Proposed Pathway for Formation of the Radical Anion, [PC − CH₃ − H]•⁻ during RDD

(m/z 488 and 506),[44] allow identification of the acyl moieties while the fragments arising from radical-directed dissociation may be used to characterize the intrachain bonding motifs within the fatty acyl substituents.

RDD spectra obtained from the phosphatidylcholines PC(9Z-18:1/9Z-18:1) and PC(6Z-18:1/6Z-18:1) are compared in Figure 2 and show clear differences arising from different double bond positions within each isomer that are absent in conventional negative ion CID mass spectra obtained from the same compounds (see Supporting Information, Figure S1c,d). The rich fragmentation present in the RDD spectra, particularly within the mass range from 550 to 800 Da, can be rationalized as

arising from radical-directed processes. For example, the intense ion signal at m/z 725 is assigned as loss of •N(CH₃)₂ from the phosphocholine headgroup, which is likely due to β-scission from an α-phosphate radical. Other product ions in this region result from intrachain carbon−carbon bond cleavages giving rise to a series of alkyl radical (e.g., C₆H₁₃•, C₇H₁₅•, etc.) or alkene (e.g., C₆H₁₂, C₇H₁₄, etc.) losses. The spacing between adjacent peaks in these spectra is typically 14 Da, which is consistent with cleavages at different methylene positions on the fatty acyl chain. An exception occurs for PC(9Z-18:1/9Z-18:1) in the spacing between the peaks at m/z 642 and 630 that correspond to neutral losses of the alkyl •C₉H₁₉ and alkenyl •C₁₀H₁₉ radicals, respectively. Here a spacing of 12 Da results (indicated by the ♦ symbols in Figure 2a) that coincides with the 9Z-double bond position in this lipid and an analogous feature is observed for the 6Z-double bond in the RDD spectrum of the PC(6Z-18:1/6Z-18:1) isomer (Figure 2b). Scission of the double bond has been observed previously in the high energy CID fragmentation of unsaturated fatty acids and has been proposed to proceed via rearrangement of the double bond.[45] Although the mechanisms of product ion formation here are not completely understood, some plausible unimolecular dissociation pathways that account for the significant fragmentation behaviors are provided as Supporting Information (see Schemes S1−S3). Irrespective of mechanism however, the diagnostic peak spacing of 12 Da at the site of the double bond provides for the unambiguous assignment of this structural feature in these phosphatidylcholine isomers. Indeed, this pattern of peak spacing (i.e., 12 Da at the double bond location and 14 Da otherwise) has been used successfully to differentiate double bond isomers in unsaturated fatty acid derivatives using EI[28] and high energy CID.[46]

Other phospholipid classes were also found to form complexes with IB, such as phosphatidylethanolamine (PE) and phosphatidylserine (PS). It was noted however, that in the absence of the fixed charge present in PC the noncovalent complexation to PE and PS was not as efficient and adduct ions incorporating sodium, such as [M − H + Na + IB]⁻ were found to be more abundant. PD of these complexes gave rise to radical anions derived from either loss of atomic iodine or concomitant loss of iodine and benzoic acid (see Supporting Information Figure S2a and S3a). It was found that subsequent CID of either the [M − H + Na + IB − I]•⁻ or the [M − H + Na − H]•⁻ product ions could yield structurally diagnostic RDD spectra (Supporting Information Figures S2b and S3b, respectively). In both cases patterns of alkyl radical losses similar to those obtained with PC were observed and the characteristic peak spacing of 12 Da corresponding to the site of unsaturation was preserved.

The fixed charge, trimethylammonium moiety in sphingomyelins (SM) means this class is also amenable to complexation with iodobenzoate. PD of the adduct ion [SM(d18:1/9Z-18:1) + IB]⁻ at m/z 975 gave rise to the loss of I• to form a radical anion at m/z 848 (see Supporting Information Figure S4a). Subsequent CID performed on this odd electron species results in the demethylated sphingomyelin radical ion [SM − CH₃ − H]•⁻ at m/z 712 due to the neutral loss of methyl benzoate (Supporting Information Figure S4b). The spectrum arising from further CID of this ion (Figure 2c) yields RDD processes with a series of alkyl radical losses including two distinctive pairs of "doubled peaks". The first such pattern at m/z 585 results in a 12 Da spacing between fragments arising from chain cleavage at the C9 and C10 positions analogous to the sequence for the monounsaturated oleoyl chain in PCs. While m/z 585 is consistent with the 127 Da neutral loss of a saturated •C₉H₁₉
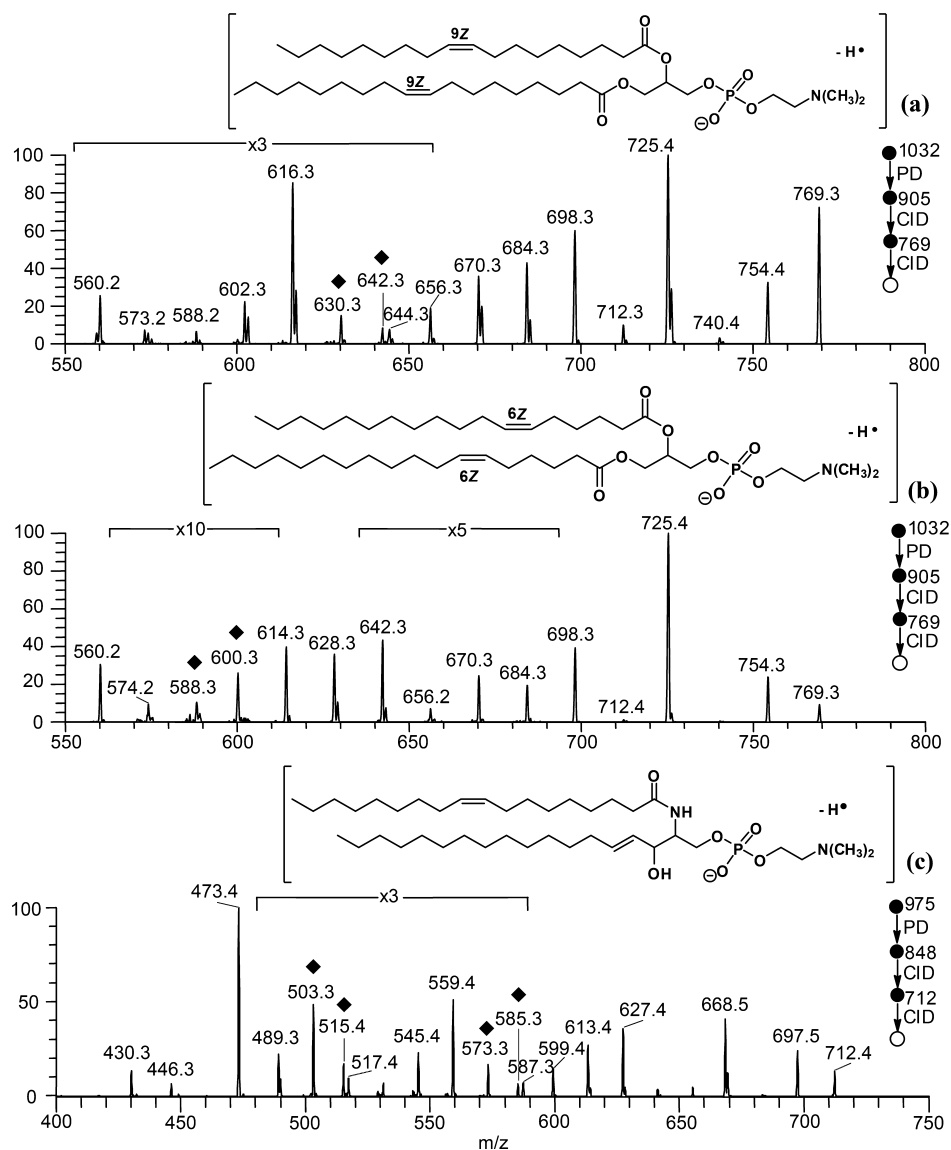
Figure 2. RDD mass spectra acquired from [PC + IB]$^-$ adducts for (a) PC(9Z-18:1/9Z-18:1), (b) PC(6Z-18:1/6Z-18:1), and (c) SM(d18:1/9Z-18:1). Product ions with a distinctive spacing of 12 Da are labeled with symbols (♦) and coincide with the positions of double bonds in each case.

radical, the companion ion at m/z 587 results from the 125 Da neutral loss of an unsaturated $^\bullet C_9H_{17}$ radical. Both processes require some unimolecular rearrangement prior to dissociation and proposals are outlined in the Supporting Information (Scheme S2−S3). Importantly however, the same pattern is reflected in all Δ^9-unsaturated phospholipids investigated here including PC(9Z-18:1/9Z-18:1) (Figure 2a), PE(16:0/9Z-18:1) (Supporting Information Figure S2b) and PS(16:0/9Z-18:1) (Supporting Information Figure S3c). As noted earlier, the RDD spectrum of SM(d18:1/9Z-18:1) reveals two examples of this phenomenon, namely, that just discussed which is associated with the Δ^9-double bond on the oleoyl chain and a second such feature with peaks at m/z 515 and 517 arising from neutral losses of 197 and 195 Da, respectively. The latter can be attributed to ejection of a saturated ($^\bullet C_{14}H_{29}$) and an unsaturated ($^\bullet C_{14}H_{27}$) radical with cleavage of the carbon−carbon double bond in the sphingosine backbone. This example, combined with data from the Δ^9-phospholipids, suggests a general trend in the radical-induced dissociation at the positions of unsaturation in phospholipids. The spectrum obtained for PC(6Z-18:1/6Z-

18:1) (Figure 2b) is an exception, however, only showing the product ion resulting from loss of the saturated $^\bullet C_{12}H_{25}$ radical (m/z 600) with no prominent companion ion at m/z 602. This may reflect a change in mechanism but could also be a symptom of the overall lower signal-to-noise ratio of these features in the spectrum of this isomer. Finally, the RDD spectrum of the sphingomyelin reveals an intense peak at m/z 473 (Figure 2c) for which no analogous signals are observed in the glycerophospholipids investigated thus far. This ion corresponds to a neutral loss of the $C_{15}H_{29}{}^\bullet CHOH$ from the sphingosine backbone and represents a useful marker for the sphingomyelin lipid class. Together these data suggest that RDD is a sensitive probe for the identification and characterization of sphingomyelins. Importantly, this approach provides for unambiguous assignment of double bond positions within these molecules allowing, among other things, differentiation of sphingomyelins from isomeric dihydrosphingomyelins.

The capacity of RDD to distinguish differing substitution patterns within saturated fatty acid substituents was also examined. Specifically, the behavior of saturated nonbranching
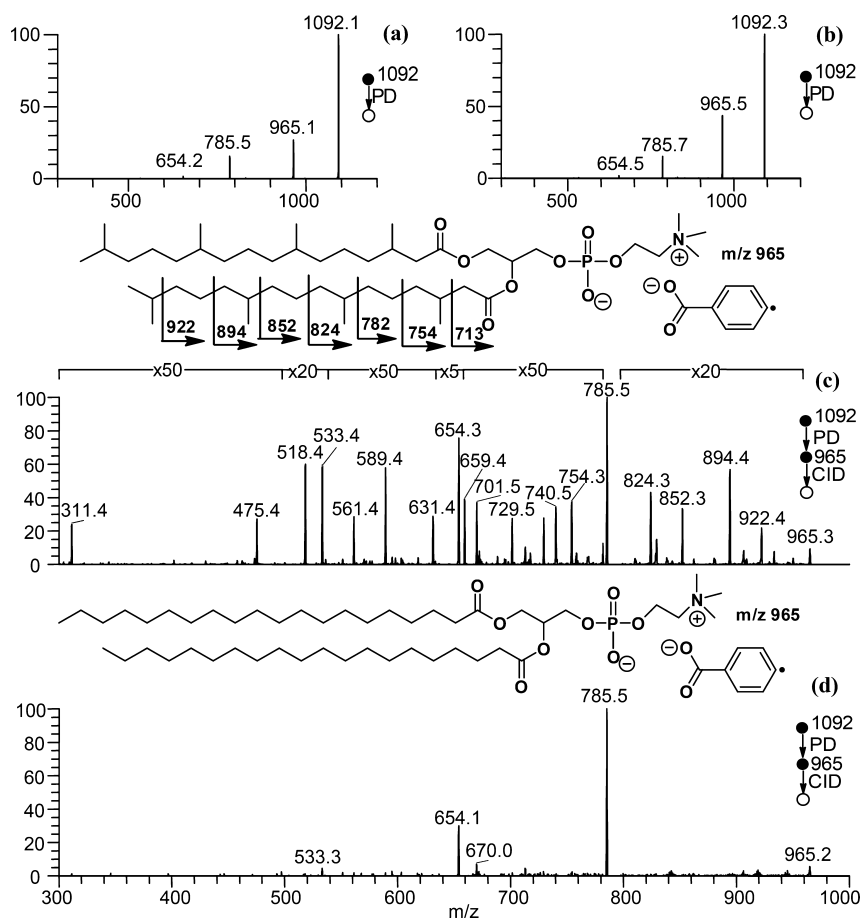
Figure 3. PD spectra of (a) [PC(20:0/20:0) + IB]⁻ and (b) [PC(4Me16:0/4Me16:0) + IB]⁻. RDD spectra from (c) PC(4Me16:0/4Me16:0) and (d) PC(20:0/20:0). Note that the same magnifications indicated in spectrum c are also applied to d.

arachidoyl (20:0) moiety was compared to that of the branched phytanoyl (4Me16:0) substituents in isomeric PCs. Once again, where such isomeric chain motifs are present within complex lipids, conventional CID spectra of the even-electron precursor ions yield identical product ions (see Supporting Information, Figure S5). Shown in Figure 3a and b are PD spectra of the isomeric [PC + IB]⁻ adduct ions that each reveal radical ion products corresponding to [PC + IB − I]•⁻ at m/z 965. Unlike the unsaturated PCs discussed above, subsequent CID of these radical anions does not result in demethylation of the phosphatidylcholine (i.e., [PC − H − CH₃]•⁻ are not observed). Instead, the spectra in Figure 3c and d are dominated by the product ion at m/z 785 corresponding to the combined neutral loss of methyl benzoate and the dimethylaminyl radical. The neutral loss of fatty acyl chains as hydrogen deficient radicals (i.e., 311 Da) is also observed at m/z 654 although at significantly lower abundance. The presence of these product ions in the RDD spectra of both PCs suggest that in the absence of the activated allylic hydrogens present in unsaturated lipids, initial hydrogen atom abstraction can occur from either the headgroup (giving rise to m/z 785) or the glycerol backbone (giving rise to m/z 654). In addition to these product ions, the RDD spectrum of PC(4Me16:0/4Me16:0) (Figure 3c) reveals an array of low abundance product ions that clearly differentiate it from its straight chain isomer (Figure 3d). Closer examination of this fragmentation pattern reveals that these product ions arise from neutral losses corresponding to the alkyl radicals: •C₃H₇, •C₅H₁₁, •C₈H₁₇, •C₁₀H₂₁, •C₁₃H₂₇, and •C₁₅H₃₁. The presence of these

features in the RDD spectrum of the diphytanoyl isomer and their absence in the diarachidoyl species is consistent with greater propensity for hydrogen atom abstraction from the tertiary carbons present in these acyl chains of the former. Indeed, the formation and fate of radicals at the branching positions can account for the dissociation observed in Figure 3c that arises from either (i) β-scission from tertiary radicals located at the branching points (e.g., β-scission from a C11-tertiary radical gives the m/z 894 product ion with a neutral loss of •C₅H₁₁) or (ii) ejection of a tertiary radical by cleavage adjacent to the branching point (e.g., dissociation of the C10−C11 bond leads to the m/z 852 product ion with the neutral loss of •C₈H₁₇ incorporating the C11-tertiary radical). The pattern of alkyl radical losses in the RDD spectrum is thus diagnostic of the positions of the four methyl branching groups on C16:0 backbone of phytanoyl substituents. This predictable fragmentation behavior suggests that such patterns can be used to identify the position(s) of chain branching where such motifs are present in complex lipids complementing the recent observations for simple lipids by EI-CID.[32]

Ionization of nonpolar TG lipids is commonly achieved by adduct formation with ammonium or sodium cations during ESI.[47,48] Protonated 4-iodoaniline (IA) is therefore a convenient noncovalent radical initiator for TGs as it incorporates the ammonium functional group, the aromatic chromophore and the photolabile C−I bond. Noncovalent complexes were thus prepared by ESI of methanolic solutions of TG and IA. Conventional CID of [TG + IA]⁺ complexes resulted in the

loss of iodoaniline to form protonated TG, as well as loss of iodoaniline coupled with neutral losses of fatty acid substituents (data not shown) directly paralleling the reported behavior of $[TG + NH_4]^+$ adduct ions.[47] In contrast, photodissociation mass spectra of $[TG + IA]^+$ complexes show loss of atomic iodine resulting in odd-electron product ions, for example, m/z 925 for TG(16:0/16:0/9Z-18:1) (Figure 4a) and m/z 951 for TG(16:0/
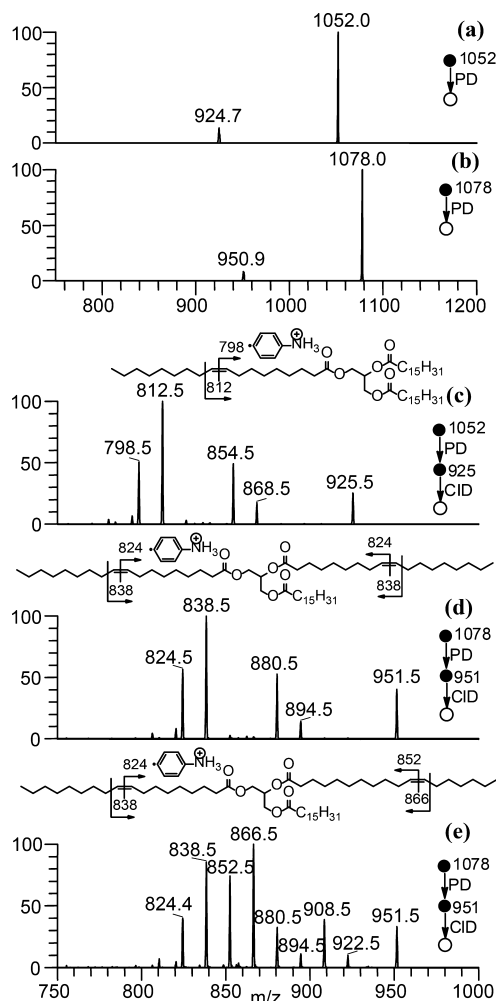

Figure 4. PD spectra of (a) [TG(16:0/16:0/9Z-18:1) + IA]$^+$ and (b) [TG(16:0/9Z-18:1/9Z-18:1) + IA]$^+$. RDD spectra obtained from [TG + IA]$^+$ complexes for (c) TG(16:0/16:0/9Z-18:1), (d) TG(16:0/9Z-18:1/9Z-18:1), and (e) TG(16:0/11Z-18:1/9Z-18:1).

9Z-18:1/9Z-18:1) (Figure 4b). Subsequent CID of these radical ions does not give rise to neutral loss of aniline but rather radical-directed dissociation of the unsaturated acyl chains is observed (Figure 4c–e). For example, RDD spectra from the Δ^9-unsaturated lipids TG(16:0/16:0/9Z-18:1) and TG(16:0/9Z-18:1/9Z-18:1) both show four abundant product ions arising from neutral loss of the alkyl radicals $C_4H_9{}^\bullet$, $C_5H_{11}{}^\bullet$, $C_8H_{17}{}^\bullet$, and $C_9H_{19}{}^\bullet$ (Figures 4c and d). While the equivalent product ions also arise from the analogous Δ^9-double bond in TG(16:0/11Z-18:1/9Z-18:1), an additional quartet is observed — offset by 28 Da — indicative of the Δ^{11}-position of unsaturation (Figure 4e). These data suggest a predictability that can be used to elucidate double bond position in unsaturated TGs (see later) but also hint at the central role of this motif in the RDD process. One possible rationale for this fragmentation is outlined in Scheme 2, wherein

Scheme 2. Proposed Pathway for RDD of $[TG + IA]^+$ Complexes[a]
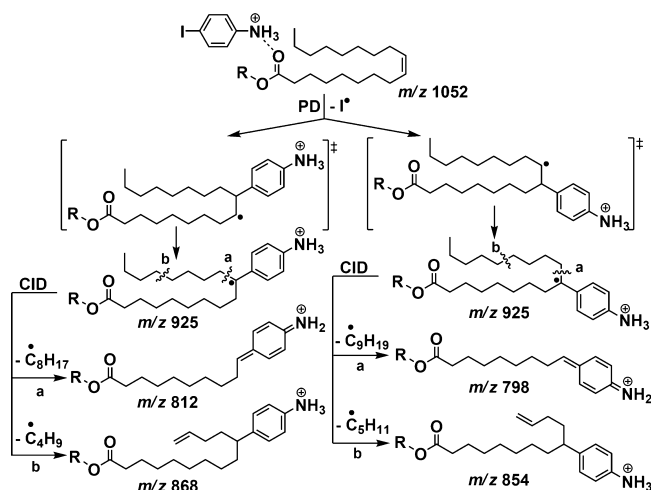
[a] The m/z values correspond to Figure 4c.

the nascent phenyl radical, unmasked by photodissociation, undergoes facile addition to the carbon–carbon double bond. On the basis of precedent from peptide RDD results, the radical is expected to swiftly migrate to a stabilized position such that the putative structures for the radicals ultimately isolated are benzylic species. Given that the initial addition can occur at either of the sp^2-carbons, two isomeric benzyl radicals are possible with subsequent dissociation accounting for the four major product ions with two products from each position of attachment. The presence of the anilinium moiety in each of the four products and the absence of any abundant product ions arising from neutral or charged aniline supports the proposition of covalent bond formation between the charge carrier and the lipid. The precise mechanism for radical rearrangement and subsequent dissociation are likely to be complex and are the subject of ongoing investigations.

RDD using the iodoaniline agent was used to examine TGs in several biologically derived lipid extracts. Figure 5a shows the RDD mass spectrum of the $[TG(50:1) + IA]^+$ adduct ion formed from ESI of an unfractionated olive oil extract in the presence of iodoaniline. Four of the major product ions observed in this spectrum (i.e., m/z 868, 854, 812, and 798) are identical to those observed in the analogous spectrum obtained from synthetic standard of TG(16:0/16:0/9Z-18:1) (Figure 4c). Interestingly however, another set of four peaks are also observed at minor abundance (i.e., m/z 896, 882, 840, and 826) that are consistent with the neutral losses observed for the Δ^{11}-synthetic standard TG(16:0/11Z-18:1/9Z-18:1) (Figure 4e). This result suggests more than one isomer of the monounsaturated TG is present in the olive oil extract. Conventional CID of TG(50:1) from olive oil reveals that the dominant acyl chain combination includes two 16:0 and one 18:1 (~99% see Supporting Information Figure S6a). Furthermore, the relative abundances of product ions arising from neutral losses of these substituents in the CID spectra can be used in conjunction with a previously established calibration[38] to estimate the relative percentages of sn-positional isomers present in the mixture as 94% TG(16:0/18:1/16:0) and 6% TG(16:0/16:0/18:1). Combining the information derived from CID and RDD observations demonstrates that the TG(50:1) species present in the olive oil extract represent a mixture of up to four isomers including two sn-positional isomers
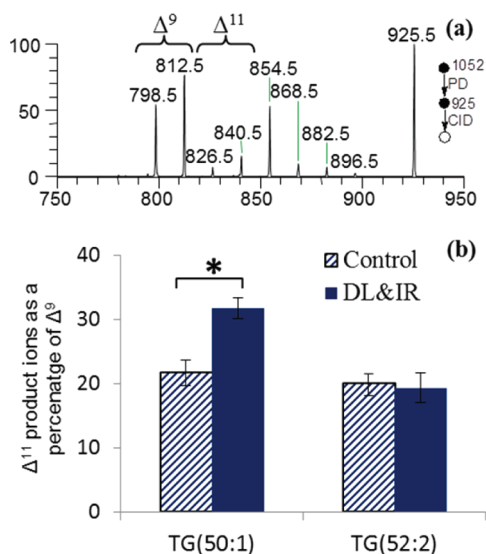
Figure 5. (a) RDD spectrum of $[TG(50:1) + IA]^+$ adduct ions at m/z 925 obtained from an olive oil extract showing product ions diagnostic of the presence of both Δ^9- and Δ^{11}-double bond positional isomers. (b) The abundance of product ions arising from Δ^{11}-double bond positional isomers plotted as a percentage of the analogous Δ^9 product ions obtained from RDD of the triacylglycerols, TG(50:1) and TG(52:2), extracted from very-low density lipoprotein (VLDL). Mean and standard deviations of measurements made for VLDL samples obtained from $n = 4$ subjects in each of two patient groups namely (i) control patients and (ii) patients with dyslipidemia and insulin resistance (DL&IR).[38] * indicates a $p < 0.05$.

as well as double bond positional variants bearing either an Δ^9-18:1 or an Δ^{11}-18:1 substituent. What cannot be directly established from these data is whether the isomeric 18:1 chains prefer a particular position on the glycerol backbone as had been inferred in other instances.[38,49]

Representative RDD mass spectra of TG(50:1) present in very-low density lipoprotein (VLDL) are provided as Supporting Information and include spectra obtained for extracts derived from (i) control patients (Supporting Information Figure S7b) and (ii) those diagnosed with dyslipidemia and insulin resistance (DL&IR) (Supporting Information Figure S7c). Both spectra were obtained under identical experimental conditions and thus the difference in abundance of the quartet of ions indicating the presence of a Δ^9-double bond and that characteristic of the Δ^{11}-double bond confirm that these features arise from mixtures of different compositions. In contrast, CID analysis of the same samples gave rise to almost indistinguishable spectra (see Supporting Information Figure S6b and c). Comparison of the ion abundances of Δ^{11}-related signals with those arising from Δ^9-double bonds was used as an indicator of variation in relative isomer populations in VLDL extracts from each of the two patient groups. This analysis was performed for the triacylglycerols, TG(50:1) and TG(52:2), and the results of this analysis are shown in Figure 5b. These data indicate that while the isomeric composition of TG(52:2) is stable between the two groups, a significant increase in the relative population of Δ^{11}-isomers is observed in DL&IR patients: a finding consistent with our previous observations of these cohorts using an independent approach.[38]

CONCLUSIONS

RDD has been demonstrated for a wide variety of complex lipids covering the major classes of glycerophospholipids, sphingomyelins and triacylglycerols. Unlike conventional CID spectra, RDD spectra obtained from complex lipids show a rich fragmentation chemistry arising from dissociation of the acyl chains and can thus be used to distinguish isomeric lipids differing in double bond position or chain-branching. The application of RDD to the analysis of biologically derived lipid extracts demonstrates the capabilities of this technology in providing information rich mass spectra directly from complex samples. While the complexity of these spectra is greater than that obtained from synthetic lipids of known structure, they provide clear evidence for the presence of multiple isomeric lipid variants at a given m/z and can even give an indication of variation in the relative abundance of these contributors. This capability has yet to be demonstrated for most of the other technologies described above and thus represents a clear advantage of the RDD approach. Ozone induced dissociation (OzID) is the exception to this, as it too has proved capable of identifying the presence of multiple isomeric lipids within complex extracts and indeed has some advantages over RDD in that it does not require formation of a special adduct ion and has fragmentation chemistry that is entirely predictable.[11] OzID is however selective for the identification of carbon−carbon double bond positions only whereas the free radical driven processes in RDD provide information on a wider array of structural variants. For example, in addition to the chain-branching demonstrated here, carbocyclic motifs and sites of oxidative lipid modification are also likely to provide diagnostic RDD fragmentation.

The ability to tailor the adducting group to suit the lipid class under investigation is also advantageous, and it is interesting to note that this results in subtle but interesting alterations in the pathways for radical ion formation. For example, for the negatively charge iodobenzoate adducts of PC and SM lipids dissociation is primarily driven by hydrogen atom abstraction (see Scheme 1), while for the positively charged iodoanilium adducts of TGs addition of the nascent radical to the sites of unsaturation accounts for most of the product ions (see Scheme 2). These differences warrant further investigation as they may suggest ways in which the dissociation chemistry can be further manipulated for greater sensitivity and selectivity of the approach.

ASSOCIATED CONTENT

⑤ Supporting Information

Experimental details and additional mass spectra are available free of charge on the Internet. This material is available free of charge via the Internet at http://pubs.acs.org.

AUTHOR INFORMATION

Corresponding Author

*E-mail: blanksby@uow.edu.au.

Present Address

¶College of Life Sciences, University of Dundee, DD1 5EH, U.K.

Author Contributions

§Authors have contributed equally.

Notes

The authors declare no competing financial interest.

■ REFERENCES

(1) Gurr, M. I.; Frayn, K.; Harwood, J. *Lipid Biochemistry*, 5th ed.; Blackwell Science: Oxford, U.K., 2002; pp 93−102.

(2) Janmey, P. A.; Kinnunen, P. K. J. *Trends Cell Biol.* **2006**, *16*, 538.

(3) Feigenson, G. W.; van Meer, G.; Voelker, D. R. *Nat. Rev. Mol. Cell Biol.* **2008**, *9*, 112.

(4) Ghosh, S.; Strum, J. C.; Bell, R. M. *FASEB J.* **1997**, *11*, 45.

(5) Gross, R. W.; Jenkins, C. M.; Yang, J.; Mancuso, D. J.; Han, X. *Prostaglandins Other Lipid Mediators* **2005**, *77*, 52.

(6) Mannock, D. A.; Lewis, R. N. A. H.; McMullen, T. P. W.; McElhaney, R. N. *Chem. Phys. Lipids* **2010**, *163*, 403.

(7) Martinez-Seara, H.; Róg, T.; Pasenkiewicz-Gierula, M.; Vattulainen, I.; Karttunen, M.; Reigada, R. *Biophys. J.* **2008**, *95*, 3295.

(8) Mukherji, M.; Schofield, C. J.; Wierzbicki, A. S.; Jansen, G. A.; Wanders, R. J. A.; Lloyd, M. D. *Prog. Lipid Res.* **2003**, *42*, 359.

(9) Jaikishan, S.; Björkbom, A.; Slotte, J. P. *Biochim. Biophys. Acta* **2010**, *1798*, 1987.

(10) Mitchell, T. W.; Pham, H.; Thomas, M. C.; Blanksby, S. J. *J. Chromatogr. B* **2009**, *877*, 2722.

(11) Brown, S. H. J.; Mitchell, T. W.; Blanksby, S. J. *Biochim. Biophys. Acta* **2011**, *1811*, 807.

(12) Krylova, I. N.; Sablin, E. P.; Moore, J.; Xu, R. X.; Waitt, G. M.; MacKay, J. A.; Juzumiene, D.; Bynum, J. M.; Madauss, K.; Montana, V.; Lebedeva, L.; Suzawa, M.; Williams, J. D.; Williams, S. P.; Guy, R. K.; Thornton, J. W.; Fletterick, R. J.; Willson, T. M.; Ingraham, H. A. *Cell* **2005**, *120*, 343.

(13) Brown, S. H. J.; Mitchell, T. W.; Oakley, A. J.; Pham, H. T.; Blanksby, S. J. *J. Am. Soc. Mass Spectrom.* **2012**, *23*, 1441.

(14) Dyer, B. S.; Jones, J. D.; Ainge, G. D.; Denis, M.; Larsen, D. S.; Painter, G. F. *J. Org. Chem.* **2007**, *72*, 3282.

(15) Rauch, J.; Gumperz, J.; Robinson, C.; Sköld, M.; Roy, C.; Young, D. C.; Lafleur, M.; Moody, D. B.; Brenner, M. B.; Costello, C. E.; Behar, S. M. *J. Biol. Chem.* **2003**, *278*, 47508.

(16) Banchet-Cadeddu, A.; Henon, E.; Dauchez, M.; Renault, J.-H.; Monneaux, F.; Haudrechy, A. *Org. Biomol. Chem.* **2011**, *9*, 3080.

(17) Han, X.; Gross, R. W. *J. Lipid Res.* **2003**, *44*, 1071.

(18) Hsu, F. F.; Turk, J. *J. Chromatogr. B* **2009**, *877*, 2673.

(19) Thomas, M. C.; Mitchell, T. W.; Deeley, J. M.; Harman, D. G.; Murphy, R. C.; Blanksby, S. J. *J. Anal. Chem.* **2007**, *79*, 5013.

(20) Moe, M. K.; Anderssen, T.; Strom, M. B.; Jensen, E. *J. Am. Soc. Mass Spectrom.* **2005**, *16*, 46.

(21) Cheng, C.; Gross, M. L.; Pittenauer, E. *Anal. Chem.* **1998**, *70*, 4417.

(22) Pittenauer, E.; Allmaier, G. *J. Am. Soc. Mass Spectrom.* **2009**, *20*, 1037.

(23) Hsu, F.-F.; Turk, J. *J. Am. Soc. Mass Spectrom.* **2008**, *19*, 1681.

(24) Hsu, F. F.; Turk, J. *J. Am. Soc. Mass Spectrom.* **2010**, *21*, 657.

(25) Castro-Perez, J.; Roddy, T. P.; Nibbering, N. M. M.; Shah, V.; McLaren, D. G.; Wang, S.-P.; Attygalle, A. B.; Chen, Z.; Johns, D. G.; Previs, S.; Vreeken, R. J.; Mitnaul, L.; Herath, K.; Hubbard, B. K.; Hankemeier, T. *J. Am. Soc. Mass Spectrom.* **2011**, *22*, 1552.

(26) Xu, Y. H.; Brenna, J. T. *Anal. Chem.* **2007**, *79*, 2525.

(27) Thomas, M. C.; Mitchell, T. W.; Harman, D. G.; Deeley, J. M.; Nealon, J. R.; Blanksby, S. J. *Anal. Chem.* **2008**, *80*, 303.

(28) Dobson, G.; Christie, W. W. *Eur. J. Lipid Sci. Technol.* **2002**, *104*, 36.

(29) Dobson, G.; Christie, W. W. *Trends Anal. Chem.* **1996**, *15*, 130.

(30) Hamilton, J. T. G.; Christie, W. W. *Chem. Phys. Lipids* **2000**, *105*, 93.

(31) Hejazi, L.; Ebrahimi, D.; Guilhaus, M.; Hibbert, D. B. *J. Am. Soc. Mass Spectrom.* **2009**, *20*, 1272.

(32) Ran-Ressler, R. R.; Lawrence, P.; Brenna, J. T. *J. Lipid Res.* **2012**, *53*, 195.

(33) Zirrolli, J. A.; Murphy, R. C. *J. Am. Soc. Mass Spectrom.* **1993**, *4*, 223.

(34) James, P. F.; Perugini, M. A.; O'Hair, R. A. J. *J. Am. Soc. Mass Spectrom.* **2008**, *19*, 978.

(35) Yoo, H. J.; Håkansson, K. *Anal. Chem.* **2010**, *82*, 6940.

(36) Ly, T.; Julian, R. R. *J. Am. Chem. Soc.* **2008**, *130*, 351.

(37) Brohall, G.; Behre, C. J.; Hulthe, J.; Wikstrand, J.; Fagerberg, B. *Diabetes Care* **2006**, *29*, 363.

(38) Ståhlman, M.; Pham, H. T.; Adiels, M.; Mitchell, T. W.; Blanksby, S. J.; Fagerberg, B.; Ekroos, K.; Borén, J. *Diabetologia* **2012**, *55*, 1156.

(39) Ly, T.; Kirk, B. B.; Hettiarachchi, P. I.; Poad, B. L. J.; Trevitt, A. J.; da Silva, G.; Blanksby, S. J. *Phys. Chem. Chem. Phys.* **2011**, *13*, 16314.

(40) Harrison, K. A.; Murphy, R. C. *J. Mass Spectrom.* **1995**, *30*, 1772.

(41) Houjou, T.; Yamatani, K.; Nakanishi, H.; Imagawa, M.; Shimizu, T.; Taguchi, R. *Rapid Commun. Mass Spectrom.* **2004**, *18*, 3123.

(42) Zhang, X.; Reid, G. E. *Int. J. Mass Spectrom.* **2006**, *252*, 242.

(43) Blanksby, S. J.; Ellison, G. B. *Acc. Chem. Res.* **2003**, *36*, 255.

(44) Murphy, R. C.; Pulfer, M. *Mass Spectrom. Rev.* **2003**, *22*, 332.

(45) Griffiths, W. J. *Mass Spectrom. Rev.* **2003**, *22*, 81.

(46) Griffiths, W. J.; Yang, Y.; Lindgren, J. Å.; Sjövall, J. *Rapid Commun. Mass Spectrom.* **1996**, *10*, 21.

(47) McAnoy, A. M.; Wu, C. C.; Murphy, R. C. *J. Am. Soc. Mass Spectrom.* **2005**, *16*, 1498.

(48) Murphy, R. C.; James, P. F.; McAnoy, A. M.; Krank, J.; Duchoslav, E.; Barkley, R. M. *Anal. Biochem.* **2007**, *366*, 59.

(49) Deeley, J. M.; Thomas, M. C.; Truscott, R. J. W.; Mitchell, T. W.; Blanksby, S. J. *Anal. Chem.* **2009**, *81*, 1920.